Received: 16 July 2018 | Revised: 13 September 2018 | Accepted: 14 September 2018

DOI: 10.1111/azo.12276

Check for updates

ORIGINAL ARTICLE

WILEY Acta Zoologica

Comparative hindlimb bone morphology in noctilionid fisher bats (Chiroptera: Noctilionidae), with emphasis on *Noctilio leporinus* postnatal development

Juan Sebastian Celeita[1] | **Nicolás Reyes-Amaya**[2] | **Adriana Jerez**[3]

[1]Departamento de Biología, Universidad Nacional de Colombia, Bogotá, Colombia

[2]Unidad Ejecutora Lillo (CONICET – Fundación Miguel Lillo), San Miguel de Tucumán, Argentina

[3]Laboratorio de Ecología Evolutiva, Departamento de Biología, Universidad Nacional de Colombia, Bogotá, Colombia

Correspondence
Nicolás Reyes-Amaya, Unidad Ejecutora Lillo (CONICET - Fundación Miguel Lillo), San Miguel de Tucumán, Argentina.
Email: nrreyesa@unal.edu.co

Funding information
Consejo Nacional de Investigaciones Científicas y Técnicas (CONICET), Grant/Award Number: PICT 2012-1583 and PICT 2015-2389

Abstract

The hindlimbs allow bats to attach to the mother from birth, and roost during independent life. Despite the great morphological diversity in Chiroptera, the hindlimbs morphology and its postnatal development have been poorly studied. Postnatal development of hindlimbs in *Noctilio leporinus* is described, further comparing the morphology of adults with that of *Noctilio albiventris* and previously reported species (*Desmodus rotundus*, *Artibeus lituratus*, *Molossus molossus*). The ossification ending sequence at autopodium elements of *N. leporinus* does not follow the distal to proximal directional sequence described for *D. rotundus*, exhibiting a heterochronic delayed ossification ending for the digits of *N. leporinus* regarding other hindlimb elements, associated with the bigger relative autopodium size of this fisher bat regarding other bat species. Noctilionid bats share the same adult hindlimb bone morphology, except for differences at hindlimb proportions and calcar ossification degree. There are differences in the number and position of bony processes, slots and sesamoids of adult noctilionid fisher bats regarding previously reported species; most differences are concentrated at the autopodium and are related to an increased surface for muscular insertion and the structural support of claws. These facts seem to be closely associated with functional demands of the feeding strategy of noctilionid fisher bats.

KEYWORDS

bone process, bulldog bats, hindlimbs, ossification, sesamoids

1 | INTRODUCTION

Bats (Chiroptera) comprise approximately 1,300 species grouped into 20 families, being one of the most diverse groups of mammals (Amador, Moyers-Arévalo, Almeida, Catalano, & Giannini, 2016; Fenton & Simmons, 2015) and exhibiting numerous specializations at the sensory, motor and behavioural systems, enabling this group to encompass a large number of nocturnal niches (Denzinger & Schnitzler, 2013). In addition, this group of mammals is the only one that has developed an active flight, presenting a particular body plan associated with this ability (Scholey, 1986; Walton & Walton, 1970). Thus, the limbs of these animals demonstrate a balance between adequate structural support and weight reduction for flight, involving particular morphological patterns such as bone reductions and rotation of the joints (MacAlister, 1872; Vaughan, 1959), passive digital lock (Schutt, 1993) and the presence of calcar in some species (Schutt & Simmons, 1998).

Neotropical fisher bats (Noctilionidae) comprise the genus *Noctilio*, which groups the sympatric species *Noctilio leporinus* and *Noctilio albiventris* (Pavan, Martins, & Morgante,

 © 2018 The Royal Swedish Academy of Sciences

2012). The external and cranial morphology of these species is similar (Hood & Jones, 1984). However, *N. leporinus* is larger and has a diet based mainly on fish, crustaceans and eventually insects (Bordignon, 2006; Brooke, 1994); whereas *N. albiventris* has a smaller size, with a diet based on insects, and occasional consumption of fish (Gonçalves, Munin, Costa, & Fischer, 2007).

The factors involved in the origin of the morphological and functional diversity present in adult bats remain unknown for most species (Reyes-Amaya & Jerez, 2013). The relationship between feeding habits and morphology in piscivorous bats has focused mainly on the cranial structure (Curtis & Santana, 2018; Santana & Cheung, 2016), while the study of the postcranial morphology of the genus has been focused on its taxonomic implications (Schutt & Simmons, 1998). Studies on morphology and its ontogenetic variations in the postcranium of Chiroptera have focused on the forelimbs and in embryonic stages (Bishop, 2008), whereas the postnatal development of the hindlimbs has been approached in very few species despite the great morphological diversity of bats (Reyes-Amaya, Jerez, & Flores, 2017). The particular ecological characteristics of *N. leporinus* make it an ideal taxon to make morpho-functional comparisons with other species of different ecological habits. The objective of this study was to describe the morphology and postnatal development of the hindlimbs of *N. leporinus* in relation to the ecology and feeding habits of this species, further comparing the definitive characteristics present in the adult of *N. leporinus* with those of adults of *N. albiventris* (this study) and previously reported species with different ecological habits (*Desmodus rotundus*, *Artibeus lituratus*, *Molossus molossus*, Reyes-Amaya et al., 2017).

2 | MATERIALS AND METHODS

2.1 | Sampling and processing of specimens

For the description of the postnatal development of hindlimb bony elements in *N. leporinus*, six specimens from a postnatal ontogenetic series were used. For the description of comparative hindlimb bone morphology in adults of species with different ecological habits, one specimen of *N. leporinus* and one specimen of *N. albiventris* were used, also including previous descriptions of *D. rotundus*, *A. lituratus*, and *M. molossus* (Reyes-Amaya et al., 2017). The specimens of *N. albiventris* and *N. leporinus* were borrowed from the mammal collection of the Instituto Alexander Von Humboldt (IAvH) and the mammal collection Alberto Cadena García (ICN, Instituto de Ciencias Naturales, Universidad Nacional de Colombia), respectively. The specimens were cleared and double-stained for bone and cartilage according to Wassersug (1976). We did not attempt to evaluate sex as a variable source due to the small sample size.

2.2 | Age categories, anatomical nomenclature and morphological descriptions

For all descriptions, the nomenclature of the bones, bone processes and sesamoids followed Schaller (2007), Nomina Anatomica Veterinaria (World Association of Veterinary Anatomists, 2012) and Reyes-Amaya et al. (2017). The regions described correspond to the stylopodium (sty: femur), zeugopodium (zp: tibia and fibula) and autopodium (ap), the latter being composed of basipodium (bp: tarsals), metapodium (mp: metatarsals) and acropodium (acp: phalanges). Because the exact age of specimens was unknown, the developmental staging of the sample followed Reyes-Amaya and Jerez (2013), based on morphological (suture closure), morphometric (forearm length) and reproductive (sexual maturity) characters. Six stages of development (B to F, and H) grouped into three age categories (juvenile to adult) were recognized at the sample, as follows: juvenile (B, $n = 1$; C, $n = 1$; D, $n = 1$; E, $n = 1$), subadult (F, $n = 1$) and adult (H, $n = 1$) (Table 4).

Ossification sequence and greatest changes in shape, position and spatial relationship among bony elements were described for the postnatal development of *N. leporinus*, also describing general changes in the shape of the hindlimb as well as the zeugopodium/autopodium (zp/ap) and the stylopodium/zeugopodium (sty/zp) length ratios. In addition, the definitive adult morphology of the hindlimbs of *N. leporinus* was compared with the morphology of *N. albiventris* and the previously described for species with different ecological habits (Reyes-Amaya et al., 2017): *Desmodus rotundus*, *Molossus molossus* and *Artibeus lituratus*. All descriptions were made via stereomicroscope observations.

3 | RESULTS

3.1 | Postnatal development of hindlimbs in *N. leporinus*

3.1.1 | Stage B (juvenile)

The hindlimb exhibits a relatively robust appearance, with a zeugopodium that exceeds the stylopodium length (sty/zp ratio 0.88; Table 4) and an autopodium that exceeds both the stylopodium and the zeugopodium length (zp/ap ratio 0.92; Table 4; Figure 1a). Except for the calcar, all bony elements have already begun the ossification process (Table 1).

Stylopodium: At the femur, the diaphysis is completely ossified, exhibiting elliptical shape in cross section, while the proximal and distal epiphyses each exhibit a secondary ossification centre and the greater trochanter process exhibit an own ossification centre. The proximal epiphysis of the femur exhibits a dorsal sesamoid in ossification process (called here

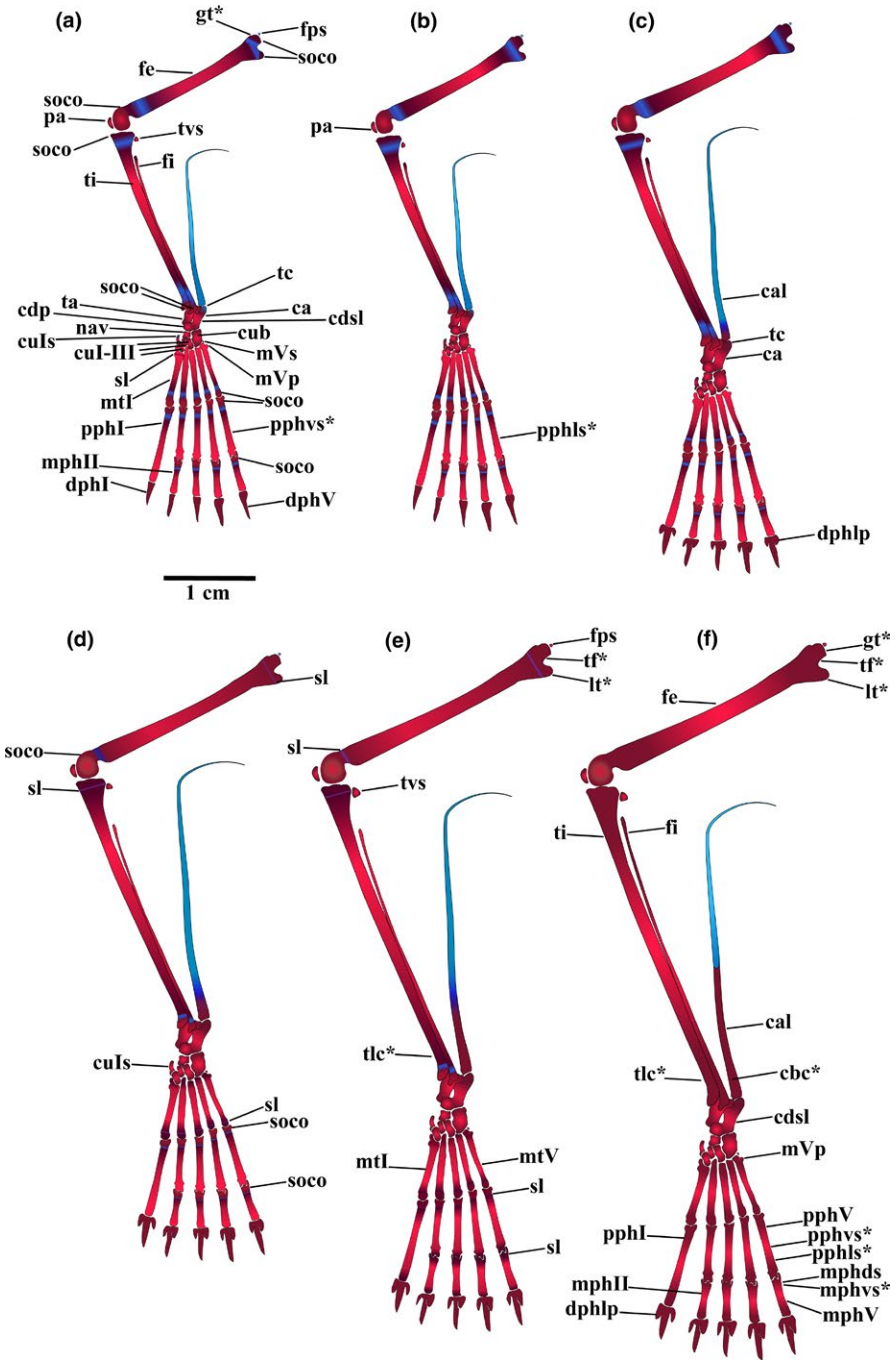

FIGURE 1 General diagrams of the hindlimbs of *Noctilio leporinus* at dorsal view along postnatal development. (a) juvenile B stage of development. (b) juvenile C stage. (c) juvenile D stage. (d) juvenile E stage. (e) subadult F stage. (f) adult H stage of development. ca: calcaneous; cal: calcar; cbc: calcar basal crest; cdp: calcaneous dorsal process; cdsl: calcaneous dorsal slot; cub: cuboid; culs: cuneiform I ventral sesamoid; cuI-III: cuneiforms I to III; dphI: distal phalange I; dphlv: distal phalanges lateral process; dphV: distal phalange V; fi: fibula; fe: femur; fps: femur proximal sesamoid; mphII: medial phalange II; mphV: medial phalange V: mphds, medial phalanges dorsal slots; mphvs: medial phalanges ventral slots; mtI: metatarsal I; mtV: metatarsal V; mVp: metatarsal V proximal process; mVs: metatarsal V ventral sesamoid; nav: navicular; nvp: navicular ventral process; pa: patella; pphI: proximal phalange I; pphls: proximal phalanges lateral slots; pphV: proximal phalange V; pphvs: proximal phalanges ventral slots; oco: ossification centre open; sl: suture line; soco: secondary ossification centre open; ta: talus; tc: tuber calcanei; tf: trochanteric fossa; gt: greater trochanter; ti: tibia; lt: lesser trochanter; tlc: tibial lateral crest; ttp: trochlea tali proximalis; tvs: tibial ventral sesamoid. Asterisk "*" indicates structures present but not visible at dorsal view

as femur proximal sesamoid), while the distal epiphysis of the femur exhibits dorsally the patella in ossification process (Table 2).

Zeugopodium: The diaphysis of the tibia is completely ossified, exhibiting elliptical shape in cross section, while the proximal and distal epiphyses each exhibit a secondary ossification centre. The proximal epiphysis of the tibia exhibits ventrally the tibial ventral sesamoid (Table 2). The fibula extends parallel and straight from the distal tip of the tibia up to approximately 4/5 of its length. The diaphysis of the fibula is completely ossified, being approximately five times thinner than that of the tibia, while the distal epiphysis exhibits a secondary ossification centre. The proximal end of the fibula does not show evidence of epiphysis or secondary ossification centre.

Autopodium: At the basipodium level, all elements are completely ossified, except for the calcaneus (still in ossification process) and the calcar (cartilaginous in this stage; Table 1). The calcar exhibits an extremely elongated and slightly depressed shape. The talus is rectangular and slightly compressed, with a central constriction. The trochlea tali proximalis process appears for the first time and completely developed at the proximal end of the talus, articulating with the tibia and fibula (Table 3). The calcaneus exhibits an

TABLE 1 Ossification sequence of hindlimb bony elements in a postnatal series of *Noctilio leporinus*. For each bony element, the first appearance of the "x" symbol indicates the first inkling of ossification. The second appearance of the "x" symbol indicates end of ossification, including the closure of secondary ossification centres, if present

Region		Bony elements	Neonate–prenatal	Juvenile				Subadult	Adult
				B	C	D	E	F	H
Stylopodium		Femur	x						x
Zeugopodium		Fibula	x						x
		Tibia	x						x
Autopodium	Basipodium	Talus	x	x					
		Calcaneus	x			x			
		Calcar				x			x
		Navicular	x	x					
		Cuneiform I	x	x					
		Cuneiform II	x	x					
		Cuneiform III	x	x					
		Cuboid	x	x					
	Metapodium	Metarsal I	x					x	
		Metarsal II	x					x	
		Metarsal III	x					x	
		Metarsal IV	x					x	
		Metarsal V	x					x	
	Acropodium	Proximal phalange I	x						x
		Proximal phalange II	x						x
		Proximal phalange III	x						x
		Proximal phalange IV	x						x
		Proximal phalange V	x						x
		Medial phalange II	x						x
		Medial phalange III	x						x
		Medial phalange IV	x						x
		Medial phalange V	x						x
		Distal phalange I	xx						
		Distal phalange II	xx						
		Distal phalange III	xx						
		Distal phalange IV	xx						
		Distal phalange V	xx						

elongated and irregular shape, with a concave and widened distal end articulating with the cuboid and navicular bones. The tuber calcanei process (round and compressed in articulation with the calcar base) starts its development at the proximal end of the calcaneus exhibiting an own ossification centre, while the calcaneous dorsal process is observed for the first time and completely developed at the distal end of the calcaneus (as a projection at the distal end of the calcaneus extending laterally over the distal portion of the talus; Table 3). Additionally, the calcaneus exhibits a dorsal slot at its centre, starting development (called here as calcaneous dorsal slot, Table 3). The cuboid exhibits a slightly triangular shape. The navicular exhibits a slightly squared shape, with the navicular ventral process completely developed extending proximally over the ventral surface of the talus (Table 3). The cuneiforms I–III have a slightly rectangular shape. The cuneiform I exhibits at its lateral end the cuneiform I ventral sesamoid. At the metapodium level, the diaphyses of the metatarsals I–V are already ossified. The distal epiphyses of metatarsals I–V presents a secondary ossification centre, while the proximal epiphysis of the metatarsal I exhibits a suture with its diaphysis, evidencing the previous existence of a secondary ossification centre at this position. The metatarsal V proximal process (which extends and widens medially and laterally the proximal epiphysis of the metatarsal V) stars its development at the proximal

TABLE 2 Ossification sequence of hindlimb sesamoids in a postnatal series of *Noctilio leporinus*. Sesamoids without name given previously in the literature are indicated with a cross symbol "†". For each sesamoid, the first appearance of the "x" symbol indicates the first inkling of ossification. The second appearance of the "x" symbol indicates end of ossification

			Juvenile				Subadult	Adult
Region	**Sesamoids**	**Neonate – Prenatal**	**B**	**C**	**D**	**E**	**F**	**H**
Stylopodium	Femur proximal sesamoid†	x					x	
	Patella	x		x				
Zeugopodium	Tibial ventral sesamoid	x					x	
Autopodium	Cuneiform I ventral sesamoid	x				x		
	Metatarsal V ventral sesamoid	x	x					

epiphysis of the metatarsal V (Table 3). The metatarsal V ventral sesamoid is exhibited for the first time completely ossified ventrally at the proximal epiphysis (Table 2). At the acropodium level, the diaphyses of all proximal and medial phalanges are already ossified, whereas the proximal epiphyses of the proximal phalanges I-V and the medial phalanges II-V exhibit a secondary ossification centre. The proximal phalange I is elongated, conferring this digit a length nearly equal to the other digits. The proximal and distal epiphyses of the proximal phalanges I-V exhibit ventrally a developing slot (called here as proximal phalanges ventral slots; Table 3). The distal phalanges are completely ossified and morphologically modified to support strong and keratinized claws (Table 1).

3.1.2 | Stage C (Juvenile)

The sty/zp ratio slightly increased (0.91; Table 4), but the zp/ap ratio is retained (0.92), showing an autopodium that still exceeds the stylopodium and zeugopodium lengths (Figure 1b).

Autopodium: At the basipodium level, the cuneiform I ventral sesamoid is more displaced towards the lateral edge of the autopodium. At the metapodium level, the proximal epiphysis of the metatarsal I is fused to its diaphysis, with no evidence of the secondary ossification centre or suture with the diaphysis. At the acropodium level, the diaphyses of the proximal phalanges I-V are compressed and exhibit a pair of distal lateral slots, forming a pair of canals at the distal end of the diaphysis (called here as proximal phalanges lateral slots).

3.1.3 | Stage D (Juvenile)

The zeugopodium emphasizes its greater length in relation to the stylopodium (sty/zp ratio 0.82), and for the first time and from now on will exceed the stylopodium and autopodium lengths (zp/ap ratio 1.05; Table 4; Figure 1c).

Autopodium: At the basipodium level, the calcaneus is completely ossified (Table 1). The tuber calcanei process is completely developed, with its own ossification centre closed (Table 3). The calcar starts its ossification process at its proximal end. At the acropodium level, the distal phalanges I–V exhibits for the first time a pair of calcified plates extending parallel at the medial and lateral sides of the distal phalanges (called here as distal phalanges lateral process, Table 3), giving this bone elements a general trident-shaped appearance (calcified plate—distal phalange—calcified plate).

3.1.4 | Stage E (Juvenile)

The sty/zp ratio increased to 0.89 and the zp/ap ratio increased to 1.07 (Table 4 Figure 1d).

Stylopodium: The proximal epiphysis of the femur is completely ossified, but there is still visible a suture with its diaphysis.

Zeugopodium: The proximal epiphysis of the tibia is completely ossified, but there is still visible a suture with its diaphysis.

Autopodium: At the basipodium level, the cuneiform I ventral sesamoid is completely ossified (Table 2). At the metapodium level, the distal epiphyses of the metatarsals I-V are completely ossified, but there is still visible a suture with the diaphyses. At the acropodium level, the distal phalanges lateral process exhibits a more advanced ossification degree, accentuating the trident-shaped appearance of the distal phalanges I-V.

3.1.5 | Stage F (Subadult)

The zeugopodium emphasizes its greater length in relation to the stylopodium (sty/zp ratio of 0.83) and autopodium lengths (zp/ap ratio of 1.30; Table 4; Figure 1e).

Stylopodium: The distal epiphysis of the femur is completely ossified, but there is still visible a suture with its

TABLE 3 Formation sequence of hindlimb bone processes and slots in a postnatal series of *Noctilio leporinus*. Bone processes without name given previously in the literature are indicated with a cross symbol "†". For each bone process, the first appearance of the "x" symbol indicates start of formation. The second appearance of the "x" symbol indicates end of formation

Region		Bone processes	Neonate – prenatal	Juvenile				Subadult	Adult
				B	C	D	E	F	H
Stylopodium		Trochanter (greater)		x					x
		Trochanter (lesser)						x	x
		Trochantric fossa						x	x
Zeugopodium		Tibial lateral crest †						x	x
Autopodium	Basipodium	Calcar basal crest †							xx
		Trochlea tali proximalis	x	x					
		Tuber calcanei		x	x				
		Calcaneous dorsal slot †		x					x
		Calcaneous dorsal process	x	x					
		Navicular ventral process	x	x					
	Metapodium	Metatarsal V proximal process		x					x
	Acropodium	Proximal phalanges lateral slots †			x				x
		Proximal phalanges ventral slots †		x					x
		Medial phalanges dorsal slots †							xx
		Medial phalanges ventral slots †							xx
		Distal phalanges lateral process †				x			xx

diaphysis. The femur proximal sesamoid ends its ossification in this stage. The lesser trochanter process and the trochanteric fossa start its development (Table 3).

Zeugopodium: On the dorso-lateral surface of the tibia, a bony crest starts its development, extending along the lateral surface of the tibia, from one-third way of the diaphysis length to its distal end (called here as tibial lateral crest; Table 3). The tibial ventral sesamoid is completely ossified (Table 2).

Autopodium: At the basipodium level, the calcar is ossified to approximately 1/4 of its total length. At the metapodium level, the distal epiphyses of the metatarsals I-V are completely fused to its diaphysis, with no evidence of the secondary ossification centres or sutures with the diaphyses, marking the end of the ossification process for these bony elements. At the acropodium level, the proximal epiphyses of the proximal phalanges I-V and the proximal epiphyses of the medial phalanges II-V are completely ossified, but there is still visible a suture with its diaphysis. At the distal phalanges I-V, the distal phalanges lateral process increases in length regarding the distal phalanges length, accentuating the trident-shaped appearance of these phalanges.

3.1.6 | Stage H (Adult)

The hindlimb exhibits a relatively robust appearance, but with a zeugopodium length exceeding the stylopodium (sty/zp ratio 0.82) and autopodium lengths (zp/ap ratio 1.31; Table 4; Figure 1f). At this stage, all bony elements and sesamoids are completely ossified (Tables 1and 2), and all bone processes are completely developed (Table 3).

Stylopodium: The proximal and distal epiphyses of the femur are fused to the diaphyses, with no evidence of the secondary ossification centres or sutures with the diaphyses, marking the end of the ossification process for this bony element (Table 1). Likewise, the greater and lesser trochanters of the femur are fully developed as is the trochanteric fossa (Table 3).

Zeugopodium: The proximal and distal epiphyses of the tibia are fused to the diaphyses, with no evidence of the secondary ossification centres or sutures with the diaphyses, marking the end of the ossification process for this bony element (Table 1). The tibial lateral crest is completely developed (Table 3). The distal epiphysis of the fibula is fused to its diaphysis, with no evidence of the secondary ossification centre or suture with the diaphysis, marking the end of the ossification process for this bony element (Table 1). The fibula extends parallel and straight from the distal tip of the tibia up to approximately 9/10 the length of the tibia.

Autopodium: At the basipodium level, the calcaneous dorsal slot is completely developed (Table 3). The calcar is completely ossified, extending its ossification to approximately 1/2 of its total length, with its remaining extension staying at cartilaginous state. The calcar exhibits for the first time and

TABLE 4 Stylopodium/zeugopodium and zeugopodium/autopodium length ratios for a postnatal series of *Noctilio leporinus* and for the adult of *Noctilio albiventris*. Collection ID of the specimens is given in parentheses

Species	Age categories	Stage of development	Stylopodium	Zeugopodium	Autopodium	sty/zp	zp/ap
N. leporinus	Juvenile	B (ICN 2253)	18.88	21.58	23.44	0.88	0.92
		C (ICN 2241)	20.46	22.58	24.68	0.91	0.92
		D (ICN 2239)	22.08	26.85	25.68	0.82	01.05
		E (ICN 2252)	25.84	29.04	27.21	0.89	01.07
	Subadult	F (ICN 2246)	29.21	35.01	27.05	0.83	1.29
	Adult	H (ICN 2248)	29.66	36.05	27.40	0.82	1.32
N. albiventris	Adult	H (IAvH−8084)	18.74	18.97	14.14	0.99	1.34

Note. sty: stylopodium; zp: zeugopodium; ap: autopodiumMeasurements in millimetres

completely developed the calcar basal crest, as a prominent biconcave keel that extends along the proximal portion of the lateral surface of the calcarr (Table 3). At the metapodium level, the metatarsal V proximal process is completely developed (Table 3). At the acropodium level, the proximal epiphyses of the proximal phalanges I-V and the proximal epiphyses of the medial phalanges II-V are completely fused to its diaphysis, with no evidence of the secondary ossification centres or sutures with the diaphyses, marking the end of the ossification process for these bony elements. The proximal phalanges lateral slots and the proximal phalanges ventral slots are completely developed (Table 3). The distal epiphyses of the medial phalanges I-V exhibit for the first time and completely developed a dorsal and a ventral slot (called here as medial phalanges dorsal slots and medial phalanges ventral slots, respectively; Table 3). The distal phalanges lateral process is completely developed, extending parallel to the distal phalanges I-V up to 1/2 of its length, defining its final trident-shaped appearance (Table 3).

3.2 | Comparative adult hindlimb morphology of *Noctilio leporinus* and *Noctilio albiventris*

The hindlimbs of the adults of *Noctilio leporinus* and *Noctilio albiventris* share the same bone elements and bone morphology (Figure 1 and 3). However, the hindlimb of *N. albiventris* is markedly smaller and exhibits slightly higher sty/zp (0.99) and zp/ap (1.34) ratios than those found in *N. leporinus* (sty/zp 0.82, zp/ap 1.32; Table 4, Figure 3b). At the autopodium, for the basipodium level, the calcar of *N. albiventris* is ossified up to 1/3 of its total length, while the calcar of *N. leporinus* is ossified up to 1/2 of its total length (Figure 3b). At the autopodium, for the acropodium level, the distal phalanges lateral process of *N. albiventris* is extended 1/4 of the length of the distal phalanges, being less developed than in *N. leporinus*, where it reaches 1/2 of the length of the distal phalanges (Table 5; Figure 3d,e).

4 | DISCUSSION

4.1 | Postnatal development of Hindlimbs in *N. leporinus*

The hindlimb autopodium of the early juvenile B stage of *N. leporinus* (the earlier stage at this sample) represents a well-developed structure that has already reached 85.55% of its definitive adult length (Table 4; Figure 1a). This early development of the autopodium in bats is related to the requirements of clinging to the mother and roosting places using the hindlimbs (Farnum, Tinsley, & Hermanson, 2008; Koyabu & Son, 2014; Reyes-Amaya et al., 2017).

Although the zeugopodium/autopodium (zp/ap) length ratio of *N. leporinus* at the early juvenile B stage (0.92; Table 4) is bigger than that reported for *D. rotundus* at the same developmental stage (0.74, revealing a bigger relative size of the autopodium at *D. rotundus*), this relation is modified during the postnatal development to match the zp/ap ratios of both species at the early subadult F stage (1.29), finally exhibiting a bigger zp/ap ratio for *D. rotundus* (1.46) regarding *N. leporinus* (1.32; revealing a bigger relative size of the autopodium at *N. leporinus*) at the adult H stage (Table 4; Reyes-Amaya et al., 2017). These developmental zp/ap ratios are associated with a bigger hindlimb autopodium (relative to the zeugopodium) at the fisher bat *N. leporinus*, which use the autopodium directly to acquire and handle the food (Bordignon, 2006; Brooke, 1994), in comparison with the common vampire bat *D. rotundus*, which use the autopodium during the terrestrial locomotion (Altenbach, 1979).

The ossification onset events of the autopodium elements of several bats (see Koyabu & Son, 2014) and the ossification ending events of the autopodium elements of *D. rotundus* (Reyes-Amaya et al., 2017) have been described as a sequence with distal to proximal direction, starting with the acropodium, followed by the metapodium and ending with the basipodium elements. However, the autopodium of *N. leporinus* describes a reverse pattern for the ossification ending events, where the basipodium elements ends the ossification

process first, followed by the metapodium and ending with the acropodium elements (Table 1). This reverse pattern reveals a heterochronic shift at the ossification ending events of the hindlimb autopodium of *N. leporinus*, with the metapodium (metatarsals) and acropodium (phalanges) elements ossifying for a longer time in relation to the basipodium elements. Such heterochronic shift is associated with the highly developed autopodium (especially the digits) shown by adult specimens of *N. leporinus* (Table 5) in relation to the functional role of this structure to capture the prey (fishes); taking into account that heterochronic shifts at developmental sequences leads to evolutionary changes of trait size (Koyabu et al., 2011; Maxwell & Larsson, 2009; Sánchez-Villagra, Goswami, Weisbecker, Mock, & Kuratani, 2008).

Likewise, the ossification onset of the calcar of *N. leporinus* occurs at the juvenile D stage of development (Figure 1c), ending its ossification process at the adult H stage (Figure 1f) with a bony extension of 1/2 of the calcar total length (Table 1). These developmental timings differ from those reported for the calcar of *D. rotundus*, starting ossification at juvenile stage D and ending at juvenile stage E (Reyes-Amaya et al., 2017) and *A. jamaicensis*, starting and ending the ossification process prenatally (Adams & Thibault, 2000). These developmental timings reveal a heterochronic shift at the ossification onset and the ossification ending events for this structure, favouring a longer ossification time for the calcar of *N. leporinus* regarding other species. Such heterochronic shifts in the ossification timings of the calcar are not surprising, considering the morphological and functional diversity of this structure (Adams & Thibault, 2000; Schutt & Simmons, 1998); the bigger sized calcar of the fisher bat *N. leporinus* (Figure 1f) is strongly committed in the food handling during hunting, whereby flexing the hindlimbs, calcar (and associated uropatagium) and spine, the prey is passed from the paws to the snout (Hood & Jones, 1984).

The development of the tuber calcanei process with an own ossification centre in *N. leporinus* (at the proximal end of the calcaneus; Figure 1a) coincides with the findings previously reported for the common vampire bat *D. rotundus* (Reyes-Amaya et al., 2017). This congruence reinforces the hypothesis that this structure constitutes a traction epiphysis whereby the *m. gastrocnemius* and the *Mm. extensores breves* are inserted and originated (respectively) to extend the autopodium and its digits (Vaughan, 1959). Traction epiphyses are projections present in some bone epiphyses of mammals and birds into which a muscle is inserted and involved in mechanical movements (Parsons, 1904). Such ossifications are originated by the fusion of a pre-existing intratendinous sesamoid to the bone during evolution, showing a separate ossification centre during development (Barnett & Lewis, 1958; Parsons, 1904, 1905, 1908).

The sesamoids observed at the hindlimb of *N. leporinus* starts its ossification at early developmental stages (neonate

TABLE 5 Comparison of hindlimb bone characters in *Noctilio leporinus*, *Noctilio albiventris* (this study), *Desmodus rotundus*, *Molossus molossus* and *Artibeus lituratus* (Reyes-Amaya et al., 2017). Check symbol "✓" indicates the presence of a character, dash symbol "–" indicates the absence of a character. Sesamoids, bone processes and slots without a name given previously in the literature are indicated with a cross symbol "†". Zeugopodium/autopodium values are averages of the individual values for each species

Region	Bony elements	Characters	Species			
			Desmodus rotundus	**Molossus molossus**	**Artibeus lituratus**	***N. leporinus* – *N. albiventris***
Zeugopodium	Tibia	Tibial medial groove	✓	–	–	–
		Tibial ventral groove	✓	–	–	–
		Tibial lateral crest †	–	–	–	✓
		Tibial ventral sesamoid	–	–	✓	✓
	Fibula	Fibular dorsal and fibular ventral grooves	✓	–	–	–
		Shape of the fibula	Sturdy, nearly as thick as the tibia, complete, straight parallel along the tibial length	Thin, complete, describing an arch along the tibial length	Thin, incomplete, straight along the tibial length up to four fifths of this	Thin, incomplete, straight along the tibial length up to nine tenths of this
		Distal fibular articulation	Articulates with the tibia, talus, and calcaneus	Articulates with the tibia and the talus	Articulates with the tibia and the talus	Articulates with the tibia, talus, and calcaneus

(Continued)

TABLE 5 (Continued)

Region	Bony elements	Characters	Species			
			Desmodus rotundus	**Molossus molossus**	**Artibeus lituratus**	***N. leporinus* – *N. albiventris***
Autopodium	Calcar	Calcar basal crest†	–	–	–	✓
		Shape of the calcar	Sturdy (short and flattened), tab-like shaped	Thin and long up to three quarters of the zeugopodium length	Thin and long up to half of the zeugopodium length	Thin and long, wider at its base and extending to the length of the zeugopodium
		Consistence of the calcar	Mostly chondral (one-third bony)	Mostly bony (one quarter chondral)	Mostly chondral (a minimum bony portion at the base)	Bony from its base to half its extension
	Calcaneous	Tuber calcanei, medial and proximal process at the calcaneus.	✓	✓	✓	✓
		Calcaneus medial process at the Tuber calcanei	–	✓	✓	-
		Medial slot at the calcaneus †	–	–	–	✓
		Calcaneous dorsal process	✓	✓	–	✓
		Calcaneous dorsal slot	–	–	–	✓
		Calcaneous dorsal sesamoid	–	✓	–	–
	Talus	Talus dorsal process	✓	✓	–	–
		Talus dorsal sesamoid	–	✓	–	–
		Talus ventral sesamoid	–	-	✓	–
	Navicular	Navicular ventral process	✓	–	–	✓
	Metatarsals	Ossa sesamoidea dorsalia, dorsal and distal on metatarsals II–V	–	–	✓	-
		Ossa sesamoidea proximalia (paired), ventral and distal on metatarsals I–V	✓	✓	✓	–
		Os sesamoideum metatarsale, ventral and proximal on metatarsal III	–	✓	–	–
		Metatarsal V proximal process	✓	✓	✓ barely noticeable	✓
		Metatarsal V proximal sesamoid	✓	-	-	✓
	Cuneiforms	Cuneiform I ventral sesamoid	✓	✓	-	-
	Phalanges	Ossa sesamoidea dorsalia, dorsal and distal on proximal phalanx I/dorsal and proximal on medial phalanges II–V/dorsal and distal on medial phalanges II–V	✓	-	✓	–
		Proximal phalanges lateral grooves†	–	–	–	✓
		Proximal phalanges ventral grooves†	–	–	–	✓
		Medial phalanges dorsal slots†	–	–	–	✓
		Medial phalanges ventral slots†	–	–	–	✓
		Distal phalanges lateral process†	✓rudimentary	✓ rudimentary	✓ rudimentary	✓ highly developed
		zp/ap ratio	1.46; conferring a slender appearance to hindlimb	1.39; conferring a robust appearance to the hindlimb	1.35; conferring a robust appearance to the hindlimb	1.32–1.34; conferring a robust appearance to the hindlimb

or prenatal), most of them ending its ossification at late juvenile E and subadult F stages, except for the metatarsal V ventral sesamoid (ending at early juvenile B stage) and the patella (ending at early juvenile C stage, Table 3). A similar pattern is observed for the development of hindlimb bone processes (which determines the final adult shape of bones); while these bone processes start its development at different postnatal stages, most of them end its development between late juvenile D and adult H stages (Table 3). Such development timings of *N. leporinus* are consistent with those reported for the common vampire bat *Desmodus rotundus*, in which the cranial sutures closure, the bone processes completion (at skull and hindlimbs) and the sesamoids ossification ending, occurs between subadult F and G stages of postnatal development (Reyes-Amaya & Jerez, 2013; Reyes-Amaya et al., 2017), coinciding with the beginning of the independent life at this vampire bat (Schmidt, Schmidt, & Manske, 1980). These results suggest the functional nature of the hindlimb sesamoids and bone processes of *N. leporinus*, ending its development between late juvenile D and adult H stages (Tables 2 and 3), and linked to the arising during ontogeny of the independent feeding behaviour using the hindlimbs at this fisher bat, in which late juveniles leave the roost with the mother to travel to feeding grounds together, staying in contact away from the roost by vocalizations (Brown, Brown, & Grinnell, 1983).

4.2 | Comparative hindlimb morphology in adults of *N. leporinus, N. albiventris, D. rotundus, A. lituratus* and *M. molossus*

The morphological comparison of the hindlimbs of adults of *N. leporinus*, *N. albiventris* (data from this study), *D. rotundus*, *M. molossus* and *A. lituratus* (Reyes-Amaya et al., 2017), exhibits that *N. leporinus* and *N. albiventris* share the same bone elements and bone morphology (Figure 3b), revealing a set of six (6) characters shared by the noctilionid fisher bats (Noctilionidae), absent in the previously examined species (Table 5):

1. The calcar basal crest (a highly developed biconcave keel that extends along the proximal portion of the lateral surface of the calcar; Figure 3c), which constitutes an increase in the origin surface for the *m. calcaneocutaneus* (adductor muscle) and the insertion surface for the *m. depressor ossis styliformis* (abductor muscle, Schutt & Simmons, 1998; Stanchak & Santana, 2018). It has been reported that the calcar bone in bats serves as structural support for the edges of the uropatagium, facilitating the use of the uropatagium as a sac to capture and/or handle the food and as a rudder in manoeuvrability during flight (Schutt & Simmons, 1998; Stanchak & Santana, 2018; Vaughan, 1959). The presence of the calcar basal crest (Tables 3 and 5) at *N. leporinus* and *N. albiventris* suggests the high importance of the uropatagium–calcar complex (and associated muscles) in noctilionid fisher bats, related to the need to contract the uropatagium during the acquisition of the prey (avoiding the friction with the water, Vaughan, 1970) and its posterior use to handle the food (Bordignon, 2006; Brooke, 1994).
2. The tibial lateral crest (extending along the lateral surface of the tibia, from one-third way of the diaphysis length to its distal end; Figure 3c), which constitutes an increase in the origin/insertion surface for the *m. extensor hallucis longus* (rotation of the autopodium craniad and dorsad), *m. gracilis* (flexion of the shank and adduction of the hindlimb), *m. semitendinosus* and *m. semimembranosus* (extension of the femur and flexion of the shank, Vaughan, 1959, 1970). The presence of the tibial lateral crest at the zeugopodium of *N. leporinus* and *N. albiventris* (and hence the marked development of its associated muscles) is congruent with the great agility and strength of the hindlimb in noctilionid fisher bats, associated with the food acquisition and posterior handling during hunting (Bordignon, 2006; Brooke, 1994).
3. The calcaneous dorsal slot (dorsal slot at the centre of the calcaneus; Figure 2a,b), which constitutes an increase in the origin surface for the *m. flexor digitorum brevis* (flexion of the digits, Vaughan, 1970).
4. The proximal phalanges lateral slots (paired distal lateral slots at proximal phalanges I–V) and the proximal phalanges ventral slots (a ventral slot at epiphyses of proximal phalanges I–V; Figure 3f), which constitutes an increase in the insertion surface for the *Mm. interossei* (flexion of the digits, Vaughan, 1959).
5. The medial phalanges dorsal slots (a dorsal slot at distal epiphyses of medial phalanges I-V) and the medial phalanges ventral slots (a ventral slot at distal epiphyses of medial phalanges I-V; Table 3, Figure 3g), which constitutes an increase in the insertion surface for the *Mm. lumbricales* (flexion of the digits, Vaughan, 1959).
6. A highly developed distal phalanges lateral process (Tables 3and 5, Figures 1f and 3a,d,e), as a pair of calcified plates extending parallel at the medial and lateral surfaces of the distal phalanges up to 1/2 its length. This bone process gives to the distal phalanges a general trident-shaped appearance (calcified plate – distal phalange – calcified plate), constituting a support structure for the extremely developed keratinized claws of *N. leporinus*, and possibly an increase in the insertion surface for the *Mm. extensores breves*, *m. extensor digitorum longus* (extension of the digits), *m. plantaris* and *m. flexor digitorum fibularis* (flexion of the digits, Vaughan, 1959, 1970). At the previously examined bat species *D. rotundus*, *A. lituratus* and *M. molossus* (Reyes-Amaya et al.,

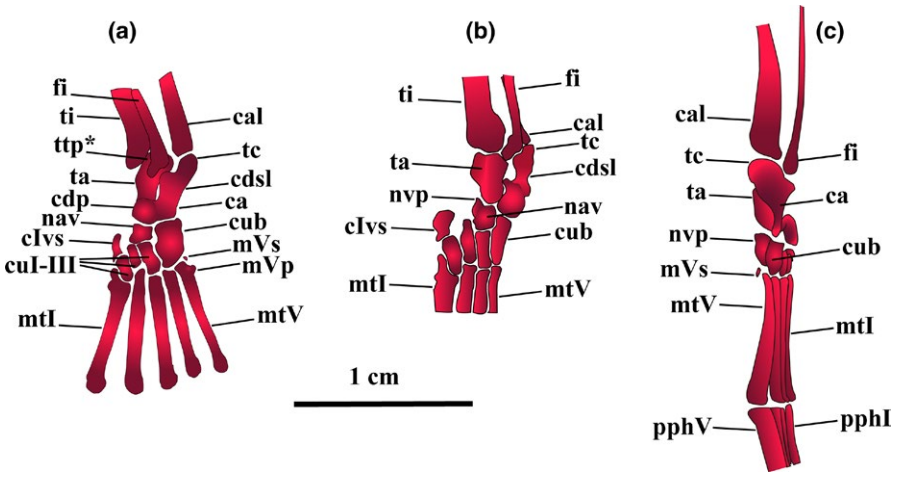

FIGURE 2 Detailed diagrams of the adult hindlimb of *Noctilio leporinus*. (a) dorsal view. (b) dorsal view with a rotation of 25°C. (c) lateral preaxial view. ca: calcaneus; cdp: calcaneous dorsal process; cal: calcar; cdp: calcaneus dorsal process; cdsl: calcaneous dorsal slot; cub: cuboid; cuIs: cuneiform I ventral sesamoid; cuI-III: cuneiforms I to III; fi: fibula; mtI: metatarsal I; mtV: metatarsal V; mVp: metatarsal V proximal process; mVs: metatarsal V ventral sesamoid; nav: navicular; nvp: navicular ventral process; pphI: proximal phalange I; pphV: proximal phalange V; ta: talus; tc: tuber calcanei; ti: tibia

2017), the distal phalanges lateral process is exhibited as a pair of rudimentary scales at just the proximal-most portion of the lateral and medial surfaces of the distal phalanges. There is a striking information gap on the morphology and development patterns of the distal phalanges and its associated claws in mammals (Ethier, Kyle,

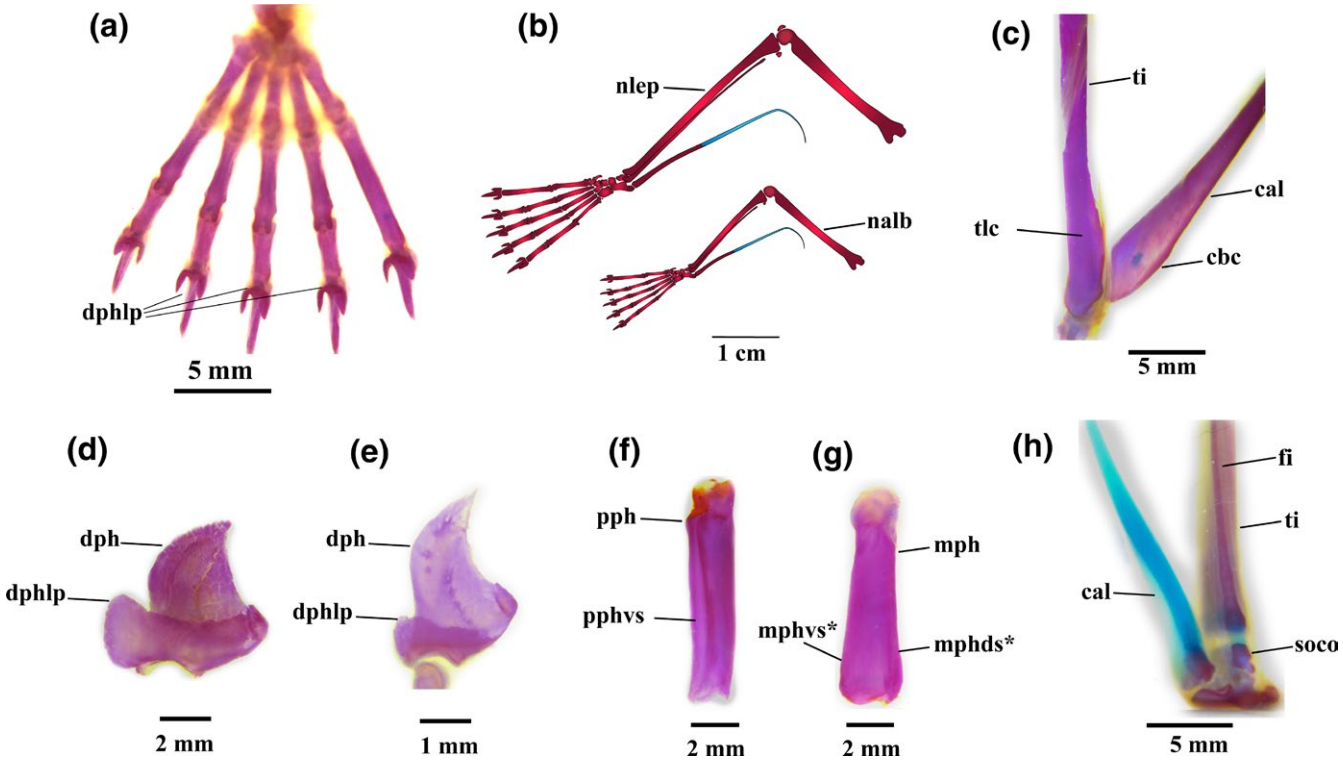

FIGURE 3 Detailed diagrams of some bone elements of the adult hindlimbs of the genus *Noctilio*. (a) dorsal view of the autopodium of *Noctilio albiventris*. (b) comparison of the hindlimb size in adults of the genus *Noctilio*. (c) zeugopodium-autopodium joint of *Noctilio leporinus*. (d) lateral view of the distal phalange of *Noctilio leporinus*. (e) lateral view of the distal phalange of *Noctilio albiventris*. (f) lateral view of the proximal phalange of *Noctilio leporinus*. (g) lateral view of the medial phalange of *Noctilio leporinus*. (h) zeugopodium-autopodium joint of *Noctilio leporinus* juvenile. ca: calcaneus; cal: calcar; cbc: calcar basal crest; dphlp: distal phalanges lateral process; fi: fibula; mph: medial phalange; nalb: *Noctilio albiventris*; nlep: *Noctilio leporinus*; oco: ossification centre open; pph: proximal phalange; ppvg; proximal phalanx ventral groove; soco: secondary ossification centre open; ti: tibia; tlc: tibial lateral crest

Kyser, & Nocera, 2010), highlighting the importance of future anatomical investigations on these structures related to the evolution and ecology of bats, since this group of mammals uses the claws to roost and obtain/handle the food.

Regarding the presence of these tarsal (calcaneous dorsal slot) and phalangeal slots (proximal phalanges lateral slots, proximal phalanges ventral slots, medial phalanges dorsal slots and medial phalanges ventral slots; Tables 3and 5), as well as the highly developed distal phalanges lateral process (Tables 3and 5) at the hindlimb autopodium of *N. leporinus* and *N. albiventris*, those structures involve a support function as well as a marked development of its associated muscles, in congruence with the great agility and strength of the autopodium (specially the digits) at these fisher bats, associated with the food acquisition and posterior handling during hunting (Brooke ,1994; Bordignon, 2006).

Likewise, the morphological comparison of the hindlimbs of adults of *N. leporinus*, *N. albiventris* (data from this study; Figure 3b), *D. rotundus*, *M. molossus* and *A. lituratus* (Reyes-Amaya et al., 2017) reveals a set of nine (9) characters shared by the noctilionid fisher bats (Noctilionidae) and some of the previously examined species (Table 5):

1. A smaller zp/ap length ratios present at *N. leporinus* (1.32), *N. albiventris* (1.34; Table 4, Figure 3b), *A. lituratus* (1.35) and *M. molossus* (1.39), regarding *D. rotundus* (1.46; Reyes-Amaya et al., 2017). These hindlimb proportions reveal an adaptive greater autopodium length (relative to the zeugopodium) at bats that use their hindlimbs (especially the autopodium) directly to acquire and/or handle the food (*N. leporinus* and *N. albiventris*, fish; *A. lituratus*, fruits; *M. molossus*, insects) in comparison to the common vampire bat (Table 5). These hindlimb proportions also reinforce the hypothesis of a slender hindlimb in *D. rotundus* adults (due to a bigger zeugopodium in relation to the autopodium length) favouring the terrestrial locomotion at this vampire bat with a mechanical advantage during walking (Reyes-Amaya et al., 2017), in which the zeugopodium length represents the distance of the step taken with the hindlimb by extending the knee (Altenbach, 1979).
2. An incomplete development of the fibula in *N. leporinus*, *N. albiventris* (Figure 3b) and *A. lituratus* (Reyes-Amaya et al., 2017; Schutt & Simmons, 2006). This characteristic is consistent with the complete development, robustness and associated muscles of the fibula of *D. rotundus* and *M. molossus* in relation to its frequent terrestrial locomotion, regarding the absence of terrestrial locomotion in *A. lituratus* (Reyes-Amaya et al., 2017)and the occasional terrestrial locomotion in *N. leporinus* and *N. albiventris* (authors personal observations).
3. The calcaneous dorsal process (as a projection at the distal end of the calcaneus extending laterally over the distal portion of the talus; Figure 2a) in *N. leporinus*, *N. albiventris*, *D. rotundus* and *M. molossus* (Reyes-Amaya et al., 2017; Table 5). The function of this bone process in *N. leporinus* and *N. albiventris* could be associated to a robust articulation of the calcaneus with the talus, dealing with the mechanical stress involved in hunting fish with the hindlimbs. Likewise, this bone process could be associated with the occasional terrestrial locomotion of *N. leporinus* and *N. albiventris* (authors personal observations); taking into account that the presence of the calcaneous dorsal process in *D. rotundus* and *M. molossus* has been suggested as a character that grants a greater stability to the hindlimbs of these species during walking (Reyes-Amaya et al., 2017).
4. The distal articulation of the fibula with the tibia, talus and calcaneus at *N. leporinus*, *N. albiventris* (Figures 1f and 2a) and *D. rotundus* (Reyes-Amaya et al., 2017), rather than only with the tibia and talus at *A. lituratus* and *M. molossus* (Reyes-Amaya et al., 2017).
5. The navicular ventral process at the distal end of the navicular bone (extending proximally over the ventral surface of the talus; Figure 2b,c) of *N. leporinus*, *N. albiventris* and *D. rotundus* (Reyes-Amaya et al., 2017).

Regarding the distal articulation of the fibula with the tibia, talus and calcaneus, and the presence of the navicular ventral process at *N. leporinus*, *N. albiventris* and *D. rotundus*, those characters are associated with a greater tight articulation between bony elements at the zeugopodium-autopodium joint and the basipodium. In this sense, *N. leporinus* and *N. albiventris* are dealing with the mechanical stress involved in hunting fish with the hindlimbs and also may deal with the mechanical stress involved in the occasional terrestrial locomotion at these noctilionid fisher bats, taking into account that in *D. rotundus,* these characters have been suggested as granting more stability to the hindlimbs during walking (Reyes-Amaya et al., 2017).

6. The tibial ventral sesamoid at the zeugopodium of *N. leporinus*, *N. albiventris* (Figure 1f) and *A. lituratus* (Reyes-Amaya et al., 2017), possibly associated to the mechanical stress at the hindlimb zeugopodium during the food acquisition (e.g. fish, fruit) and posterior handling, since the development of sesamoids is influenced by a combination of genetic and epigenetic factors (Sarin & Carter, 2000; Sarin, Erickson, Giori, Bergman, & Carter, 1999).
7. The metatarsal V ventral sesamoid at the autopodium of *N. leporinus*, *N. albiventris* (Figure 2a,c) and *D. rotundus* (Reyes-Amaya et al., 2017).
8. Cuneiform I ventral sesamoid at the autopodium of *N. leporinus*, *N. albiventris* (Figure 2a,b), *D. rotundus* and *M. molossus*.

Regarding the presence of the metatarsal V ventral sesamoid and cuneiform I ventral sesamoid at the autopodium of *N. leporinus* and *N. albiventris*, it suggests its relationship to the mechanical stress at the hindlimb autopodium during the food acquisition and posterior handling at these noctilionid fisher bat, since the development of sesamoids is influenced by a combination of genetic and epigenetic factors (Sarin & Carter, 2000; Sarin et al., 1999). However, it could also be associated to the occasional terrestrial locomotion of the noctilionid fisher bats (authors personal observations), taking into account that the presence of the metatarsal V ventral sesamoid and cuneiform I ventral sesamoid at *D. rotundus* and *M. molossus* have been suggested as related to the mechanical stress at the hindlimb autopodium during the terrestrial locomotion of these species (Reyes-Amaya et al., 2017).

Regarding the cuneiform I ventral sesamoid, it was initially described for *Eumops perotis* as an extra tarsal bone termed "medial tarsal" located "lying at right angles to the long axis of the tarsus" (Vaughan, 1959, 1970). This description as an extra tarsal element is not accurate since this bone element exhibits typical sesamoidal development inside tendons (Reyes-Amaya et al., 2017; Sarin & Carter, 2000; Vickaryous & Olson, 2007). However, the cuneiform I ventral sesamoid seems to show variations of its spatial location at the autopodium of bats, since in *N. leporinus*, *N. albiventris* (this study; Figures 1d and 2a,b) and *Eumops perotis* (Vaughan, 1959), it is located slightly displaced towards the lateral side of the hindlimb, regarding the location exhibited in *D. rotundus* and *M. molossus* at the ventral surface of the cuneiform I bone element (Reyes-Amaya et al., 2017).

9. A highly developed metatarsal V proximal process at *N. leporinus*, *N. albiventris* (Figures 1f and 2a), *D. rotundus* and *M. molossus*, contrasting with the barely noticeable metatarsal V proximal process of *A. lituratus* (Reyes-Amaya et al., 2017; Table 5). This metatarsal V proximal process widens the proximal epiphysis of the metatarsal V towards both lateral and medial sides, which constitutes an increase of the insertion surface for the *m. Peroneus brevis* (flex and rotate the foot) and *m. Abductor digiti quinti* (abduct the fifth digit; Vaughan, 1959, 1970); this is congruent with the great agility and strength of the autopodium (especially the digits) in *N. leporinus* and *N. albiventris*, associated to the food acquisition and posterior handling during hunting (Bordignon, 2006; Brooke, 1994), as well as supporting the great agility and strength of the autopodium of *D. rotundus* and *M. molossus* (especially the digits) associated to the terrestrial locomotion.

The particular morphological characters described occurring during *N. leporinus* postnatal development provide some insights of the ontogenetic variation of traits possibly linked to the particular feeding strategy of this noctilionid fisher bat: (1) the calcar basal crest, (2) the tibial lateral crest, (3) the calcaneous dorsal slot, (4) the proximal phalanges lateral slots and proximal phalanges ventral slots, (5) the medial phalanges dorsal slots and medial phalanges ventral slots, and (6) a highly developed distal phalanges lateral process. Likewise, the fact that the adults of *N. leporinus* (primarily feeding on fish) and *N. albiventris* (primarily feeding on insects, occasionally fish, Gonçalves et al., 2007) share the same bone elements and bone morphology (Table 5), exhibit the ecological plasticity of the species of the family Noctilionidae, despite the unique shared morphology.

However, those characters shared by adults of *N. leporinus*, *N. albiventris* (fisher bats) and the previously examined species *D. rotundus* and *M. molossus* (walker bats, Reyes-Amaya et al., 2017; Table 5) suggest the functional plasticity of these shared characters, that in *N. leporinus* and *N. albiventris* possibly act as mechanical support during fish hunting, but in *D. rotundus* and *M. molossus* possibly act as mechanical support during terrestrial locomotion: (1) a smaller zp/ap length ratios, (2) an incomplete development of the fibula, (3) the calcaneous dorsal process, (4) the distal articulation of the fibula with the tibia, talus and calcaneus, (5) the navicular ventral process, (6) the tibial ventral sesamoid, (7) the metatarsal V ventral sesamoid, (8) the cuneiform I ventral sesamoid and (9) a highly developed metatarsal V proximal process (Table 5). Likewise, these shared characters also open up the possibility to convergent evolutionary processes that could facilitate the terrestrial locomotion in relatively distant species (in evolutionary terms), taking into account that noctilionid fisher bats (Noctilionidae) occasionally walks (authors personal observations) and the ability of walking has evolved independently in some lineages of bats (Hand et al., 2009; Riskin, Bertram, & Hermanson, 2016; Riskin, Parsons, Schutt, Carter, & Hermanson, 2006).

ACKNOWLEDGEMENTS

The authors dedicate this study to the 400 (and rising) social leaders and human rights activists selectively murdered (due to its activism) in Colombia since the signing of the peace treaty and the surrender of arms by the ex-guerrilla FARC at 2016 (Defensoría del Pueblo de Colombia, 2018). The authors thank the curators Andrés Cuervo (Vertebrate Collection, at the Instituto Alexander von Humboldt, Colombia) and H. López-Arévalo (Alberto Cadena Garcia Mammal Collection, at the Instituto de Ciencias Naturales, Universidad Nacional de Colombia, sede Bogotá, Colombia) for providing access to specimens, the Laboratorio de Equipos Ópticos Compartidos (at the Departamento de Biología, Universidad Nacional de Colombia, sede Bogotá) for providing access to the optic equipments used to make the figures, and Elizabeth Geib (Writing lab, at Purdue

University, Pordue, USA) for helping with the correction of the English translation of the manuscript.

ORCID

Nicolás Reyes-Amaya http://orcid.org/0000-0001-8509-3741

REFERENCES

Adams, R. A., & Thibault, K. M. (2000). Ontogeny and evolution of the hindlimb and calcar: Assessing phylogenetic trends. In R. A. Adams, & S. C. Pedersen (Eds.), *Ontogeny, functional ecology, and evolution of bats* (pp. 316–332). New York, NY: University Press. https://doi.org/10.1017/CBO9780511541872

Altenbach, J. S. (1979). Locomotor morphology of the vampire bat, *Desmodus rotundus*. *Special Publications American Society of Mammalogists*, *6*, 1–137. https://doi.org/10.5962/bhl.title.39538

Amador, L. I., Moyers-Arévalo, R. L., Almeida, F. C., Catalano, S. A., & Giannini, N. P. (2016). Bat systematics in the light of unconstrained analyses of a comprehensive molecular supermatrix. *Journal of Mammalian Evolution*, *25*, 37–70. https://doi.org/10.1007/s10914-016-9363-8

Barnett, C. H., & Lewis, O. J. (1958). The evolution of some traction epiphyses in birds and mammals. *Journal of Anatomy*, *92*, 593–601.

Bishop, K. L. (2008). The evolution of flight in bats: narrowing the field of plausible hypotheses. *The Quarterly Review of Biology*, *83*, 153–169. https://doi.org/10.1086/587825

Bordignon, M. O. (2006). Diet of the fishing bat *Noctilio leporinus* (Linnaeus; Mammalia, Chiroptera) in a mangrove area of southern Brazil. *Revista Brasileira De Zoologia*, *23*, 256–260. https://doi.org/10.1590/S0101-81752006000100019

Brooke, A. P. (1994). Diet of the fishing bat, *Noctilio leporinus* (Chiroptera: Noctilionidae). *Journal of Mammalogy*, *75*, 212–218. https://doi.org/10.2307/1382253

Brown, P. E., Brown, T. W., & Grinnell, A. D. (1983). Echolocation, development, and vocal communication in the lesser bulldog bat, *Noctilio albiventris*. *Behavioral Ecology and Sociobiology*, *13*, 287–298. https://doi.org/10.1007/BF00299676

Curtis, A. A., & Santana, S. E. (2018). Jaw-dropping: Functional variation in the digastric muscle in bats. *Anatomical Record*, *301*, 279–290. https://doi.org/10.1002/ar.23720

Defensoría del Pueblo de Colombia (2018). *Alerta temprana 026–2018: Nota de seguimiento al informe de Riesgo 010–2017*. Retrieved from https://www.indepaz.org.co/wp-content/uploads/2018/03/AT-N%C2%B0-026-18-Defensores.pdf, Defensoría del Pueblo de Colombia, República de Colombia, Bogotá, DC.

Denzinger, A., & Schnitzler, H. U. (2013). Bat guilds, a concept to classify the highly diverse foraging and echolocation behaviors of microchiropteran bats. *Frontiers in Physiology*, *4*, 1–15. https://doi.org/10.3389/fphys.2013.00164

Ethier, D. M., Kyle, C. J., Kyser, T. K., & Nocera, J. J. (2010). Variability in the growth patterns of the cornified claw sheath among vertebrates: Implications for using biogeochemistry to study animal movement. *Canadian Journal of Zoology*, *88*, 1043–1051. https://doi.org/10.1139/Z10-073

Farnum, C. E., Tinsley, M., & Hermanson, J. W. (2008). Forelimb versus hindlimb skeletal development in the big brown bat, *Eptesicus fuscus:* Functional divergence is reflected in chondrocytic performance in autopodial growth plates. *Cells Tissues Organs*, *187*, 35–47. https://doi.org/10.1159/000109962

Fenton, M. B., & Simmons, N. B. (2015). *Bats: A world of science and mystery*. Chicago, IL: University of Chicago Press, https://doi.org/10.1086/685368

Gonçalves, F., Munin, R., Costa, P., & Fischer, E. (2007). Feeding habits of *Noctilio albiventris* (Noctilionidae) bats in the Pantanal, Brazil. *Acta Chiropterologica*, *9*, 535–538. https://doi.org/10.3161/1733-5329(2007) 9[535:FHONAN]2.0.CO;2

Hand, S. J., Weisbecker, V., Beck, R. D. M., Archer, M., Godthel, H., Tennyson, A. J. D., & Worthy, T. H. (2009). Bats that walk: A new evolutionary hypothesis for the terrestrial behaviour of New Zealand's endemic mystacinids. *BMC Evolutionary Biology*, *9*, 169–182. https://doi.org/10.1186/1471-2148-9-169

Hood, C. S., & Jones, J. K. (1984). Noctilio Leporinus. *Mammalian Species*, *216*, 1–7. https://doi.org/10.2307/3503809

Koyabu, D., Endo, H., Mitgutsch, C., Suwa, G., Catania, K. C., Zollikofer, C. P., … Sánchez-Villagra, M. R. (2011). Heterochrony and developmental modularity of cranial osteogenesis in lipotyphlan mammals. *EvoDevo*, *2*, 21. https://doi.org/10.1186/2041-9139-2-21

Koyabu, D., & Son, N. T. (2014). Patterns of postcranial ossification and sequence heterochrony in bats: Life histories and developmental trade-offs. *Journal of Experimental Zoology Part B: Molecular and Developmental Evolution*, *322*, 607–618. https://doi.org/10.1002/jez.b.22581

MacAlister, A. (1872). The myology of the Chiroptera. *Philosophical Transactions of the Royal Society of London*, *162*, 125–171.

Maxwell, E. E., & Larsson, H. C. (2009). Comparative ossification sequence and skeletal development of the postcranium of palaeognathous birds (Aves: Palaeognathae). *Zoological Journal of the Linnean Society*, *157*, 169–196. https://doi.org/10.1111/j.1096-3642.2009.00533.x.

Parsons, F. G. (1904). Observations on traction epiphyses. *Journal of Anatomy and Physiology*, *38*, 248–258.

Parsons, F. G. (1905). On pressure epiphyses. *Journal of Anatomy and Physiology*, *39*, 402–412.

Parsons, F. G. (1908). Further remarks on traction epiphyses. *Journal of Anatomy and Physiology*, *42*, 388–396.

Pavan, A. C., Martins, F. M., & Morgante, J. S. (2012). Evolutionary history of bulldog bats (genus *Noctilio*): Recent diversification and the role of the Caribbean in Neotropical biogeography. *Biological Journal of the Linnean Society*, *108*, 210–224. https://doi.org/10.1111/j.1095-8312.2012.01979.x

Reyes-Amaya, N., & Jerez, A. (2013). Postnatal cranial ontogeny of the common vampire bat *Desmodus rotundus* (CHIROPTERA: PHYLLOSTOMIDAE). *Chiroptera Neotropical*, *19*, 1198–1211. https://doi.org/10.13140/2.1.3275.9687

Reyes-Amaya, N., Jerez, A., & Flores, D. (2017). Morphology and postnatal development of lower hindlimbs in *Desmodus rotundus* (Chiroptera: Phyllostomidae): A comparative study. *The Anatomical Record*, *300*, 2150–2165. https://doi.org/10.1002/ar.23646

Riskin, D. K., Bertram, J. E. A., & Hermanson, J. W. (2016). The evolution of terrestrial locomotion in bats. In J. E. A. Bertram (Ed.), *Understanding mammalian locomotion: Concepts and applications* (pp. 307–324). Hoboken, NJ: John Wiley & Sons. https://doi.org/10.1002/9781119113713.ch1

Riskin, D. K., Parsons, P. E., Schutt, W. A. Jr, Carter, G. G., & Hermanson, J. W. (2006). Terrestrial locomotion of the New

Zealand short-tailed bat, *Mystacina tuberculata*, and the common vampire bat, *Desmodus rotundus*. *Journal of Experimental Biology*, *209*, 1725–1736. https://doi.org/10.1242/jeb.02186

Sánchez-Villagra, M. R., Goswami, A., Weisbecker, V., Mock, O., & Kuratani, S. (2008). Conserved relative timing of cranial ossification patterns in early mammalian evolution. *Evolution and Development*, *10*, 519–530. https://doi.org/10.1111/j.1525-142X.2008.00267.x

Santana, S. E., & Cheung, E. (2016). Go big or go fish: Morphological specializations in carnivorous bats. *Proceedings of the Royal Society B: Biological Sciences*, *283*, 1–9. https://doi.org/10.1098/rspb.2016.0615

Sarin, V. K., & Carter, D. R. (2000). Mechanobiology and joint conformity regulate endochondral ossification of sesamoids. *Journal of Orthopaedic Research*, *18*, 706–712. https://doi.org/10.1002/jor.1100180505

Sarin, V. K., Erickson, G. M., Giori, N. J., Bergman, A. G., & Carter, D. R. (1999). Coincident development of sesamoid bones and clues to their evolution. *The Anatomical Record*, *257*, 174–180. https://doi.org/10.1002/(SICI)1097-0185(19991015)257:5xxaaa174:AID-AR6xxbbb3.0.CO;2-O

Schaller, O. (2007). *Illustrated veterinary anatomical nomenclature* (3rd ed.). Stuttgart, Germany: Enke Verlag.

Schmidt, C., Schmidt, U., & Manske, U. (1980). Observations of the behavior of orphaned juveniles in the common vampire bat (*Desmodus rotundus*). In D. E. Wilson, & A. L. Gardner (Ed.), *Proceedings of the fifth international bat research conference* (pp. 105–111). Lubbock, TX: Texas Tech Press.

Scholey, K. D. (1986). The evolution of flight in bats. In W. Nachtigall (Ed.), *Bat flight Fledermausflug* (pp. 1–12). New York, NY and Stuttgart, Germany: G. Fischer.

Schutt, W. A. Jr (1993). Digital morphology in the Chiroptera: The passive digital lock. *Acta Anatomica*, *148*, 219–227. https://doi.org/10.1159/000147544

Schutt, W. A., & Simmons, N. B. (1998). Morphology and homology of the chiropteran calcar, with comments on the phylogenetic relationships of Archaeopteropus. *Journal of Mammalian Evolution*, *5*, 1–32. https://doi.org/10.1023/A:1020566902992

Schutt, W. A., & Simmons, N. B. (2006). Quadrupedal bats: Form, function, and evolution. In A. Zubaid, G. F. McCracken, & T. H. Kunz (Eds.), *Functional and evolutionary ecology of bats* (pp. 145–159). New York, NY: Oxford University Press.

Stanchak, K. E., & Santana, S. E. (2018). Assessment of the hindlimb membrane musculature of bats: implications for active control of the calcar. *Anatomical Record*, *301*, 441–448. https://doi.org/10.1002/ar.23740

Vaughan, T. A. (1959). *Functional morphology of three bats: Eumops, Myotis, Macrotus*. Lawrence, Kansas: University of Kansas Publications, Museum of Natural History.

Vaughan, T. A. (1970). The skeletal system. In W. A. Wimsatt (Ed.), *Biology of bats* (pp. 97–138). New York, NY: Academic Press.

Vickaryous, M. K., & Olson, W. M. (2007). Sesamoids and ossicles in the appendicular skeleton. In B. K. Hall (Ed.), *Fins and limbs: Evolution, development and transformation* (pp. 323–341). Chicago, IL: The University of Chicago Press.

Walton, D. W., & Walton, G. M. (1970). Post-cranial osteology of bats. In R. Slaughter, & D. Walton (Eds.), *About bats* (pp. 93–125). Dallas, TX: Southern Methodist University Press.

Wassersug, R. J. (1976). A procedure for differential staining of cartilage and bone in whole formalin-fixed vertebrates. *Stain Technology*, *51*, 131–134. https://doi.org/10.3109/10520297609116684

World Association of Veterinary Anatomists (2012). *Nomina anatomica veterinaria*. Vienna, Austria: International Committee on Veterinary Anatomical Nomenclature.

How to cite this article: Celeita JS, Reyes-Amaya N, Jerez A. Comparative hindlimb bone morphology in noctilionid fisher bats (Chiroptera: Noctilionidae), with emphasis on *Noctilio leporinus* postnatal development. *Acta Zool*. 2018;00:1–15. https://doi.org/10.1111/azo.12276